Evaluation of Joint Defects on FSW of Mg Alloy using Statistical Method

T. Kinoshita[1,a], K. Hayashi[1], S. Hamada[2], I. Shigematsu[3] and H. Noguchi[2]

[1] Department of Mechanical Engineering, Graduate School of Engineering, Kyushu University
744 Moto-oka, Nishi-ku, Fukuoka 819-0395, Japan

[2] Department of Mechanical Engineering, Faculty of Engineering, Kyushu University
744 Moto-oka, Nishi-ku, Fukuoka 819-0395, Japan

[3] National Institute of Advanced Industrial Science and Technology (AIST), 2266-98 Anagahora Shimoshidami, Moriyama-ku, Nagoya 463-8560, Japan

[a] 2TE11314N@s.kyushu-u.ac.jp

Keywords: FSW, Joint defect, Statistics, Mg alloy, Fatigue limit

Abstract. To select the welding conditions that can ensure a particular fatigue strength for safe use in a structure produced by the FSW (Friction Stir Welding) of Mg alloys, this paper proposes a method for determining the range of welding conditions that can ensure a particular joint defect size limit. The welding parameters used are the rotation speed of the tool ω and the welding speed v. Generally, a welding condition is selected using only the fatigue strength as an index. However, ensuring the fatigue strength in a particular welding condition does not insure the strength and reliability of a welded part, because actual welding is not typically carried out in a particular welding condition. Therefore, a range of conditions that can ensure a particular fatigue strength is required. Moreover, we also consider parameters that represent the factors that decrease fatigue strength, namely, $\sqrt{area}$, HV, and R, because the welding conditions that can ensure a particular fatigue strength are determined by an evaluation of these factors, as well. Therefore, in this study, a method for determining a range of welding conditions that can ensure a welding defect size limit is proposed. Furthermore, FSW welding tests were carried out and the validity of the proposed method was evaluated. X-ray transmission measurements were carried out to measure the welding defect size obtained using the method. Then, the prediction of the maximum welding defect size was carried out for a welding length of 25 [m], which is representative of body of a the Shinkansen rolling stock car.

Introduction

Recently, the problem of environmental pollution caused by CO_2 exhaust and the energy problem caused by the increasing exhaustion of oil resources call for energy savings in vehicles as a solution. Among the actual materials used in vehicles, magnesium alloys are the most light-weight and have the best specific strength. Thus, we can achieve energy saving in vehicles by using Mg alloys as a structural material.

FSW (Friction Stir Welding) [1] offers many advantages such as a higher joint efficiency [2] and a lower welding cost than traditional welding technologies such as tungsten inert gas welding and metal inert gas welding. Thus, FSW is now used for welding the body of Shinkansen rolling stock car. FSW is already in practical use with aluminium alloys, though fatigue tests are carried out under various welding conditions to ensure the strength and reliability of FSW welded parts. As a result,

the practical employment of FSW with Al alloy requires a great amount of time and great expense. Moreover, because the welding process cannot actually be performed precisely in a particular condition, the strength and reliability of the welded structures are not guaranteed by the quality that was obtained in a particular welding condition.

From this background, we can see, that a range of welding conditions that can ensure a particular fatigue limit is essential for FSW to be practically applied to Mg alloys. The factors that are mainly considered to decrease the fatigue strength of an FSW welded part are welding defects, changes in crystalline structure, and residual stress. However, the welding conditions are typically determined using only fatigue limit as an index, without evaluating these other significant factors. Therefore, because the fatigue limit under various welding conditions is obtained from a fatigue test, to ensure strength and reliability, a great number of fatigue tests are needed to account for the variability involved, which in turn requires a long development time. Therefore, an evaluation of the influence of the factors that decrease the fatigue limit is required to efficiently ensure strength and reliability of FSW welded parts. The range of welding conditions that can ensure a particular value for the main factors that decrease the fatigue limit, such as joint defects, changes in crystalline structure and residual stress, are determined here, and the range of welding conditions that can ensure a particular fatigue limit can be determined using the prediction equation proposed by Murakami *et al.*[3]

$$\sigma_w = \frac{1.41(HV+120)}{\left(\sqrt{area}\right)^{1/6}}\left(\frac{1-R}{2}\right)^{\alpha} \quad (1)$$

where HV is a representative parameter of changes in a crystalline structure, $\sqrt{area}$ is a representative parameter of a joint defect, R is the stress ratio and is a representative parameter of residual stress, and α is a material constant.

Therefore, in this paper, as a first approach to evaluating fatigue limit using these three representative parameters (HV, $\sqrt{area}$, R), we determine the range of welding conditions that can ensure that a particular joint defect size is less than a given size.

Mechanism of joint defect formation

Definition of joint defect. Because FSW produces solid state joints that are different from other joints, its joint defect formation is related not only to the heat input, but also to how well the material is stirred. In a condition of insufficient heat input and stirring, a wormhole, which is a hole-shaped defect that propagates in the direction of the welding, is formed, because the materials cannot form a good joint after the tool has passed. Because a wormhole is considered to be a joint defect that is always combined with some hole-shaped defects, it is accompanied by a hole-shaped defect that is shorter in the direction than the wormhole under the condition in which a wormhole is not formed. This hole-shaped defect then becomes the origin of fracture under actual usage. Therefore in this study, such hole-shaped defects, including the wormhole, are called ‘joint defects’, and the evaluation of its defect size is carried out.

The condition of constant heat input. Because FSW produces a joint using the frictional heat produced between the tool and the material, the heat input generated from the friction is considered to be the main factor in determining the joint defect size, and this defect becomes smaller as the heat input increases. The rotation speed ω [rpm] and welding speed v [mm/min] are the welding parameters that are most generally used. In generally, the heat input per unit time during FSW is defined as ω/v [4]. This indicates that heat generation during FSW is determined by only the rotation speed ω. The heat generation during FSW welding is divided into three parts: (I) the shoulder, (II) the probe side surface, and (III) the probe bottom surface. The heat generation of (I) and (III) are

determined by the rotation speed ω, but there is another factor that is related to the heat generation of (II). The force that the probe receives from the material further ahead in the welding direction, changes as the welding speed changes, as shown in Fig. 1. The equation for the heat generation at (II) can be expressed as follows.

$$q = \mu F_D u \tag{2}$$

where q is the heat generation per unit time [J/s], μ is the friction coefficient, F_D is the resistance [N], and u is the velocity at the friction surface [m/s]. In addition, setting the radius of probe into r [m], u is represented by $u = r\omega$.

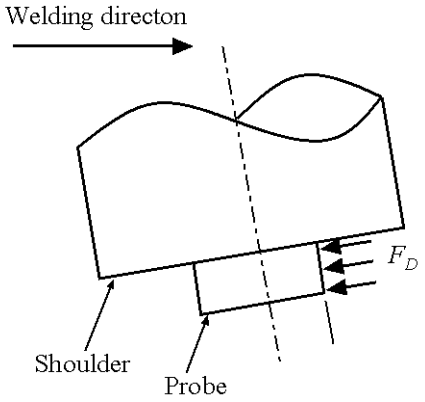

Fig. 1. Resistance experienced by the probe.

The heat generation (II) represented by Eq. 2 becomes greater as the welding speed increases, because the resistance that the probe experiences (F_D) increases as the welding speed increases. Therefore, using ω and v as the welding parameters, the condition of constant heat input is considered to be an upward convex curving line, as shown in the solid curving line in Fig. 2.

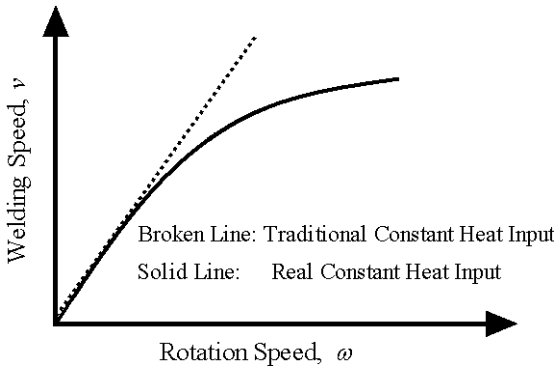

Fig. 2. Constant heat input line.

Influence of plastic flow phenomenon on joint defect formation. Schneider *et al.* [5] modelled the metal flow around a FSW probe. According to the model, the flowing metal moves around the outer circumference at the advancing side, and a vortex is formed by this movement, which has the effect of preceding the plastic flow. In addition, Shinoda *et al.* [6] tried to visualize the plastic flow phenomenon using PVC (polyvinyl chloride) to clarify the plastic flow phenomenon during FSW. They reported that a vortex that is in inverse rotation to the tool rotation arises in the direction opposite to the welding direction (going backwards), and this vortex produces the effect of stirring the material. The model of Schneider *et al.* and the report of Shinoda *et al*' present different vortex directions; in any case, to produce sufficient plastic flow, the effect of the vortex is considered to be

important. Because it is thought that the vortex is formed by the difference in pressure around the tool, it is also thought that a particular rotation speed is needed to form a sufficient vortex. Therefore, it is considered that a particular rotation speed (ω) is needed to produce fine joint.

Method of determining welding condition to ensure a particular defect size limit

Here, we determine the range of welding conditions needed to ensure a particular defect size limit. In the condition of insufficient heat input at the welded part, a joint defect is formed. Moreover, in the condition of a constant heat input as well as in the condition of a low rotation speed, the material is hard to stir, so joint defects are generated due to the insufficient plastic flow. Therefore, the range of welding conditions to ensure a particular defect size limit can be seen in the shaded area in Fig. 3. The maximum defect size that this range ensures is the maximum defect size in the condition marked by ○, in which the maximum defect size is considered to be largest in the shaded area.

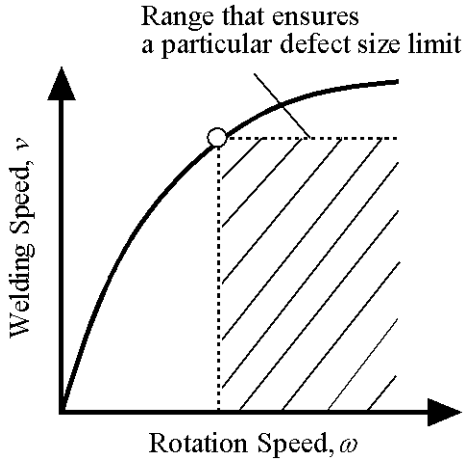

Fig. 3. Range that ensures a particular defect size limit

Method of determining ensured defect size limit

The method of determining the defect size that is ensured in the above-mentioned range is now presented. The welding condition marked by ○ is considered to be the condition within the shaded area that forms the largest defect. Therefore, the maximum ensured defect size in the shaded area shown in Fig. 3 can be determined. To predict the maximum defect size in a 25 [m] welding length, which we take as representing the body of a Shinkansen rolling stock car, we employ the statistics of extremes [7]. Measuring the defect size for use in the statistics of extremes is generally carried out by a dissection method [8], a method in which the cross-section surface is polished and observed under a microscope. However, in the statistics of extremes using the dissection method, it is necessary to cut and polish the surface for defect size measurement. In this study, then, to apply the statistics of extremes efficiently, X-ray transmission measurement is carried out. The images taken in the X-ray transmission measurements are divided into several control volumes and are organized into 3D images. The maximum defect size in the 25 [m] welding length is predicted by measuring the maximum defect size in the control volumes.

Welding tests

To evaluate the validity of a welding condition range that can ensure the determination of a particular defect size limit, FSW tests were carried out. The material used for the welding tests was extruded non-combustible magnesium alloy AMX602B (X = Ca) [9-11]. Tables 1 and 2 show the alloy's chemical composition and mechanical properties.

Table 1. Chemical composition of AMX602B (mass%)

Al	Ca	Zn	Mn	Si
5.95	1.89	0.002	0.34	0.029

Table 2. Mechanical properties of AMX602B

E [GPa]	σ_B [MPa]	HV [kgf/mm²]	σ_Y [MPa]	ε_f [%]
46	287	68	210	15

Two plates with dimensions of 120 [mm] × 50 [mm] × 2 [mm] were welded in a butt joint. Figure 5 shows the basic principle of FSW [12]. FSW was conducted with straight-line FSW test equipment produced by Hitachi Setsubi Engineering Co., Ltd. The FSW tool was made of tempered X40CrMoV5-1. The rotation direction of the tool was clock-wise, viewed from the base of the tool. The welding length was 110 [mm]. Figure 4 shows the results of the welding tests. The upper limits of the rotation speed and the welding speed of the equipment were 3000 [rpm] and 1000 [mm/min], respectively. After the welding, screening with the naked eye was carried out. It was clear that the concave welded surface caused a decrease in fatigue strength. Therefore, the welding condition in which the concave surface was regarded as irrelevant was deemed a bad welding condition, as marked by the symbol × in Fig. 5. Figure 6 shows photographs of a well-welded surface and a poorly welded surface.

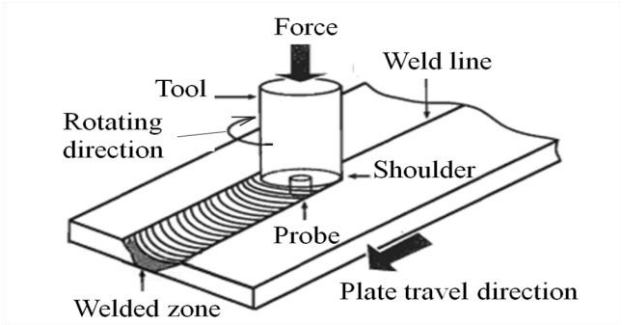

Fig. 4. Basic principle of FSW [12].

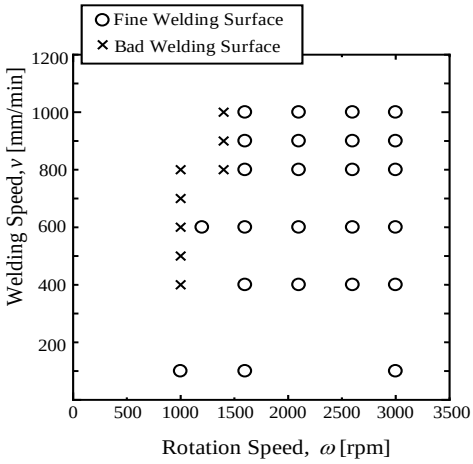

Fig. 5. Screening results of welding tests.

(a)

(b)

Fig. 6. Examples of welded surface.
(a) fine welded surface, (ω = 2100 [rpm], v = 400 [mm/min]).
(b) bad welded surface, (ω = 1400 [rpm], v = 1000 [mm/min]).

The welding condition in which the maximum defect size in the 25 [m] welding length is predicted from the statistics of extreme is an arbitrary one. However, as seen in Fig. 5, in the welding condition ω = 1600 [rpm] and v = 1000 [mm/min], the maximum defect size is considered to be the largest, because this condition has the smallest heat input and the lowest rotation speed. Then, predicting the maximum defect size in this condition is considered to be adopted. Therefore, X-ray transmission measurement was carried out on the material welded in this condition, and the defect size was measured. Figure 7 shows an example of a 3D organized image that was composed of the images taken in the X-ray transmission measurement. The areas that appear as white in Fig. 7 are the joint defects. Figure 8 shows the perspective from which Fig. 7 is seen.

Because the cross-section area of the welded part perpendicular to the welding direction is constant, the control length, *i.e.* the length that is the section for the measurement of the maximum defect size, can be used as an alternative to the control volume. The control length is 8 [mm] in this measurement. Then, because the state of both the starting point and end point is considered to be different from the steady welding state, after the welding length was divided into 14 control lengths, two control lengths on both ends were eliminated. Therefore, the maximum defect sizes were measured for a total of about 10 control lengths. The defect size $\sqrt{area}$ [3] is the root of the projected area in the direction of the load.

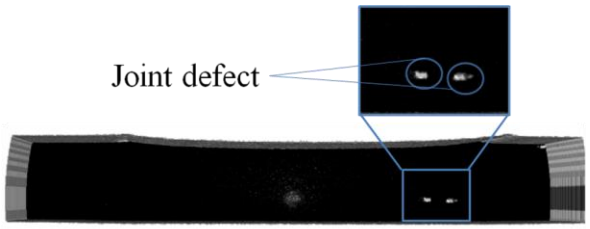

Fig. 7. Example of X-ray CT 3D image.

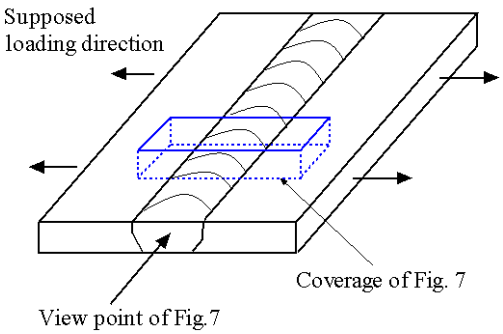

Fig. 8. View point of Fig.7.

Results and discussion

Figure 9 shows the results of the statistics of extremes using the measured maximum defect size. There were several control lengths in which the defect size could not be measured, because the maximum defect sizes were smaller than the lowest measurement limit, the maximum defect size in a 25 [m] welding length is predicted. As seen in Fig. 9, the predicted maximum defect size in a 25 [m] welding length is 670 [μm]. Therefore, the shaded range shown in Fig. 10 is the welding condition range that would ensure a 670 [μm] defect size limit in a 25 [m] welding length.

Next, we discuss the results of the tests that were carried out. The reason why the concave welding surface is considered to be the joint defect became too large, then the results of the tests indicate that the method for determining range that can ensure a particular defect size limit is valid. In addition, the validation of the predicted maximum defect size in a 25 [m] welding length and the defect size measured by X-ray transmission measurement were then carried out. The method of measuring the defect size using X-ray transmission measurement is more efficient than the existing method, which takes measurement from a cross-section surface of the material using a microscope. Then, by selecting multiple welding conditions in which the maximum defect size in a 25 [m] welding length is predicted by the statistics of extremes, the range that would ensure a particular defect size limit can be determined more precisely.

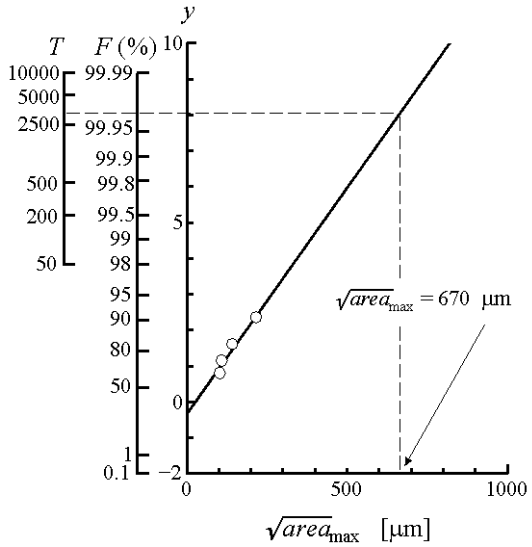

Fig. 9. Statistics of extremes of joint defects.

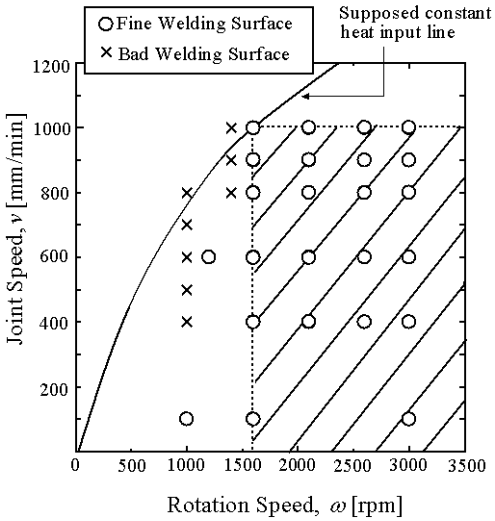

Fig. 10. Range to ensure a particular defect size limit.

Conclusion

This paper has proposed a method for determining the range of welding conditions that can ensure a particular defect size limit, using welding parameters ω and v, with consideration of the mechanism of joint defect formation. FSW tests were then carried out and the results obtained were as follows.

(1) The method of determining the range of welding conditions that can ensure a particular defect size limit is considered to be valid.

(2) By measuring the defect size using X-ray transmission measurements, the maximum defect size can be efficiently predicted.

References

[1] J. M. Thomas, E. D. Nicholas, Friction stir welding for the transportation industries, Materials & Design, Vol. 18, 4-6, (1997), p. 269.

[2] M. Ericsson, R. Sandström, Influence of welding speed on the fatigue of friction stir welds, and comparison with MIG and TIG, International Journal of Fatigue, 25 (2003), p. 1379.

[3] Y. Murakami, *Metal Fatigue*: *Effects of Small Defects and Nonmetallic Inclusions* Elsevier Science, 2002.

[4] T. Hashimoto, S. Jyogan, K. Nakata, Y.G. Kim, and M. Ushio, Proc. 1st Int. FSW Symp., Thousand Oaks, USA, 14-16 June, 1999, CD-ROM.

[5] J. Schneider, R. Beshears, A. C. Nunes. Jr., Interfacial sticking and slipping in the friction stir welding process, Materials Science and Engineering, A, 435-436 (2006), p. 287.

[6] T. Shinoda, M. Higashiyama, H. Takegami, Observations of metal flow phenomenon in friction stir welding (in Japanese), Journal of Japan Welding Society, 77 (2005-9), p. 186.

[7] E.J. Gumbel: *Statistics of Extremes*, Columbia University Press, 1963.

[8] Y. Murakami, H. Usuki, Quantitative evaluation of effects of non-metallic inclusions on fatigue strength of high strength steels, International Journal of Fatigue, 11, 5 (1989), p. 299.

[9] M. Sakamoto, S. Akiyama, T. Hagio, K. Ogi, Control of oxidation surface film and suppression of ignition of molten Mg-Ca alloy by Ca addition (in Japanese), Journal of Japan Foundry Engineering Society, 69 (1997), p. 227.

[10] S. Akiyama, H. Ueno, M. Sakamoto, H. Hirai, A. Kitahara, Development of noncombustible magnesium alloys (in Japanese), Materia Japan, 39 (2000), p. 72.

[11] S. Akiyama, Flame-Resident Magnesium Alloy by Calcium (in Japanese), Journal of Japan Foundry Engineering Society, 66 (1994), p. 38.
[12] K. Nakata, S. Inoki, Y. Nagano, T. Hashimoto, S. Jogan and M. Ushio, Weldability of friction stir welding of AZ91D magnesium alloy thixomolded sheet (in Japanese), Journal of Japan Institute of Light Metals, 51 10 (2001), p. 528.